Microsystem Technologies (2018) 24:3291–3297
https://doi.org/10.1007/s00542-018-3805-6

TECHNICAL PAPER

Low-cost surface micromachined microhotplates for chemiresistive gas sensors

K. G. Girija[1,3] · S. Chakraborty[2] · M. Menaka[4] · R. K. Vatsa[1,3] · Anita Topkar[2,3]

Received: 18 January 2018 / Accepted: 30 January 2018 / Published online: 27 February 2018
© Springer-Verlag GmbH Germany, part of Springer Nature 2018

Abstract

Microhotplate (MHP) based gas sensors have gained significant attention recently due to their small size, low power and feasibility for integration of electronics on the same chip. This study presents the detailed work on design, fabrication and complete characterization of microhotplates based on a standard multi user MEMS process (MUMPs). Suspended-membrane type MHPs were designed using the available layer combinations of MUMPs. FEM simulations were carried out to optimize the heater design by spatially varying the heater current density to achieve uniform temperature distribution over the sensing area. Topography measurements confirmed that the X–Y–Z dimensions of the fabricated MHPs were in accordance with the design. From electro-thermal characterization, the thermal efficiency of the MHPs was evaluated as ~ 10 °C/mW. The suspended membrane showed a homogeneous temperature of ~ 450 °C at 35–40 mW heater power, which was well above the typical operating temperature of chemiresistive gas sensors. The results presented in this paper provide a pathway for realizing cost effective MHPs for gas sensors based on MUMPs.

1 Introduction

Over the past few decades, significant research effort has been focussed towards the miniaturization of gas sensors and their integration with the electronics for several applications ranging from toxic gas detection to manufacturing process monitoring. Among the solid state sensors, metal oxide (MOX) gas sensors are the best suited for miniaturization since they have several advantages. These sensors are easy to fabricate, cost effective, are compatible with the silicon technology, have the ability to detect broad range of gases and are the most stable among other chemiresistive materials such as polymers and organic films (Eranna et al. 2004). To improve the selectivity, response time and reversibility in MOX sensors, the required operating temperature is usually chosen between 200 and 400 °C. This high temperature operation is required for improving the kinetics of the surface chemical reactions which induce the gas sensitivity and is the main factor which decides the power consumption of MOX gas sensors. By reducing the size of both the heater and the sensor, power consumption can be minimized to a great extent. In this regard, micro electro-mechanical systems (MEMS) based techniques are advantageous, especially for the purpose of realizing microhotplates (MHP) in order to reduce the thermal mass of MOX sensors (Kumar and Eranna 2016; Spannhake et al. 2009). Owing to their fast thermal response, MHP based gas sensors can be operated in pulsed heating mode instead of static mode, which further reduces the power consumption. The MHPs usually consist of thermally isolated membrane with an integrated heater, contact electrodes for sensing layer and sometimes a temperature sensor to measure the hotplate temperature. Due to their small size, low power consumption, ease of packaging and possibility of integration with electronics, MHPs have attracted considerable attention in the field of gas sensors (Wöllenstein et al. 2003; Bhattacharyya et al. 2008; Vernieres et al. 2017; Li et al. 2015; Rao et al. 2016). Gas sensor arrays based on different metal oxides to detect H_2, CO, NO_2 and NH_3 at 400 °C have been demonstrated by Wöllenstein et al. (2003). Nanocrystalline ZnO showed

✉ Anita Topkar
anita@barc.gov.in

[1] Chemistry Division, Bhabha Atomic Research Centre, Trombay, Mumbai 400 085, India

[2] Electronics Division, Bhabha Atomic Research Centre, Trombay, Mumbai 400 085, India

[3] Homi Bhabha National Institute, Anushaktinagar, Mumbai 400 094, India

[4] QAD Division, Indira Gandhi Center for Atomic Research, Chennai 603 102, India

enhanced response to methane at 250 °C using Ni microheater at 120 mW (Bhattacharyya et al. 2008). Vernieres et al. have reported exceptionally sensitive NO_2 sensor based on Fe nanocubes deposited on a circular MHP (Vernieres et al. 2017). MHP gas sensor based on SnO_2 hetero-structures showed high sensitivity and selectivity towards ethanol from 1 to 500 ppm range while operating at 12 mW power (Li et al. 2015). TiO_2 deposited on molybdenum microheater showed good response to CO at 500 °C at an operating power of $\sim$ 60 mW (Rao et al. 2016).

Though MHPs based on MEMS fabrication processes offer many advantages including batch processing, their fabrication is costly due to requirements of a custom fabrication process. Multi Project Wafer (MPW) runs offer a low cost solution for the development of devices based on standard silicon processes. Hence in this work, the MHPs were designed and fabricated using a commercially available, standard micromachining multi user MEMS processes (MUMPs) (Circuits Multi-Projects 2018). MUMPs provides cost effective proof-of-concept fabrication facility to research groups and universities. This enables reduction in prototyping cost and development time, in addition to optimization of design with known and tested design rules. The process is designed to be as general as possible in order to cater many different designs on a single silicon wafer. Among the three standard processes offered by MUMPs, MetalMUMPs is an electroplated nickel micromachining process. Based on MetalMUMPs, a variety of MEMS structures such as micro relay, multi-contact switches, accelerometer, gyroscope etc., have been reported (Wang and Jin 2017; Pal et al. 2015; Qu and Qu 2013; Shakoor et al. 2011). In spite of the design flexibility, microhotplates based on this process have not yet been explored. We have earlier reported initial FEM simulation results of the MHPs (Girija et al. 2015). In this paper, we present the detailed work on design, fabrication and complete characterization of microhotplates based on MetalMUMPs process.

2 Design, simulation and fabrication of MHP

Two types of heater designs based on MetalMUMPs were carried out viz. serpentine and fan shape, which are shown in Fig. 1a, b. MetalMUMPs has six mask levels and uses patterning of multiple thin film layers to form the microstructures (Girija et al. 2017). The spider like suspended-membranes of the MHP shown in Fig. 1a, b, are supported by four beams. The substrate is etched off below the membrane by forming a microtrench in order to provide very good thermal isolation. The MHP is completely processed and released from the front-side, making it more compatible with CMOS processes (Briand 2013). The membrane (300 µm × 300 µm) of the MHP consists of two silicon nitride structural layers (0.35 µm each) with an embedded poly heater (0.7 µm). Chromium–platinum layer (35 nm) is used to form inter-digitated electrodes (IDE), on which the chemical sensing layer would be deposited. Nickel–gold layer (20.5 µm) is used for the contact pads and the electrical interconnections. The membrane is suspended above a 25 µm deep trench in the silicon wafer.

Electro-thermal analysis of the MHPs is carried out using commercial FEM simulation software. The material properties and process parameters are imported from the MUMPs process file (Girija et al. 2017). The 3D solid models are meshed appropriately and electro-thermal simulation is carried out by applying a potential across the heater connections. The boundary conditions applied are (1) the substrate is fixed i.e. no mechanical movement is allowed for substrate and (2) all the heater parts including the substrate are initialised to room temperature (300 °K) at the beginning of the simulation.

Figure 1c, d show the simulated temperature profile of the MHPs for an applied voltage of 5 V. Spatial temperature uniformity is the most important requirement for any MHP. It is well reported that the inner part of the suspended membrane of the MHP experiences heat losses only due to the ambient air and radiation, whereas the outer part additionally encounters heat losses through the membrane suspension beams (Simon et al. 2001; Samaeifar et al. 2015). This causes the borders of the active area to be colder than the inner part. A popular approach to obtain temperature homogeneity is to use silicon plugs or high thermal conductivity films underneath the membrane (Graf et al. 2006). This approach is not feasible as the fabrication steps are predefined by the MUMPs process. In order to improve the temperature homogeneity, the width of the poly heater was progressively increased towards the centre from the edges (Fig. 1a, b). Thus by controlling the current density, the heater design is optimized to obtain temperature uniformity better than 10.0% over the surface comprising the IDE ($\sim$ 250 µm × 250 µm) for both the heaters. As can be seen from Fig. 1c, d, the complete MHP is heated uniformly except near the beams, which are anchoring the MHP to the substrate. The whole substrate stays nearly at ambient temperature as the suspended membrane provides good thermal isolation between the substrate and the gas-sensitive heated area. The current densities are less than 1–10 × 10^9 Am^{-2} up to a temperature of 600 °C. Beyond this temperature, electromigration effects have been reported with accompanying resistance changes attributed to redistribution of dopant species (Puigcorbe et al. 2003).

Figure 2 shows the CCD and 2D surface topography images of the fabricated MHPs with serpentine and fan

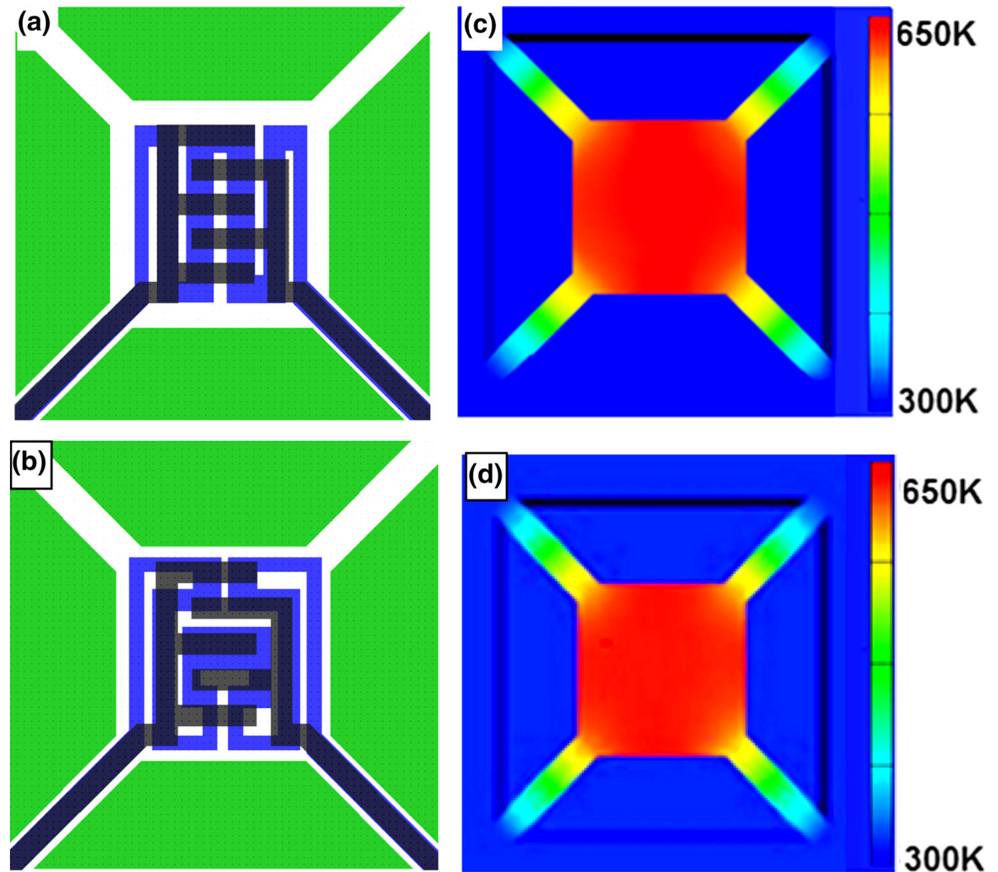

Fig. 1 2D layout of MHP with **a** serpentine and **b** fan shape heater, FEM simulation of the temperature distribution on the membrane of **c** serpentine and **d** fan shape MHP

shape heater. It is observed that the geometries match very well with the designed X–Y–Z dimensions of the MHPs. It is evident from the surface topography images that the MHP structures are suspended above the trench. These MHP chips are fixed on a PCB and the contact pads are wirebonded to the PCB using 25 µm diameter aluminum wires to facilitate the electrical characterization.

3 TCR and thermal efficiency of MHPs

It is well known that MHPs generate heat by Joule heating of the resistive heater element. The thermal energy, Q, generated by the Joule effect is given by (Briand 2013):

$$\Delta Q = RI^2 \Delta t, \tag{1}$$

where I is the current flowing through the heater resistance R during Δt time. Within a limited range of temperature, the resistivity increases linearly with temperature. The change in resistance of the poly silicon heater with temperature can be represented by (Rao et al. 2016):

$$R_T = R_o(1 + \alpha T), \tag{2}$$

where, R_T is the resistance at temperature T, R_o is the base resistance at reference temperature (usually room temperature) and α is the material property termed as the temperature coefficient of resistance (TCR). TCR can be obtained by rearranging Eq. (2):

$$\alpha = \frac{(R_T - R_0)}{R_0 T} = \frac{(\Delta R/\Delta T)}{R_0}. \tag{3}$$

TCR can be experimentally determined from the slope of the resistance of polysilicon heater vs temperature data. For this purpose, the MHP chips are mounted on a heating stage, whose temperature is precisely controlled by a PID temperature controller. The actual temperature of the MHP chips is measured by an RTD temperature sensor and the corresponding resistance value of the polysilicon heater is measured by a digital multimeter. Figure 3a shows the resistance vs temperature plot of 300 µm × 300 µm serpentine and fan MHP. From the slope of the curves, the TCR value of polysilicon is estimated as 2.6×10^{-3}/°C. The heater resistance increased linearly in the measured temperature range for both the MHPs. Thermal efficiency of the microhotplates is computed by electrically heating the polysilicon resistor with known heater power and measuring the resistance values. The heater resistance as a function of input heating power is shown in Fig. 3b. The resistance changes linearly with applied power at the rate of ~ 18 and ~ 16 Ω/mW respectively for serpentine and

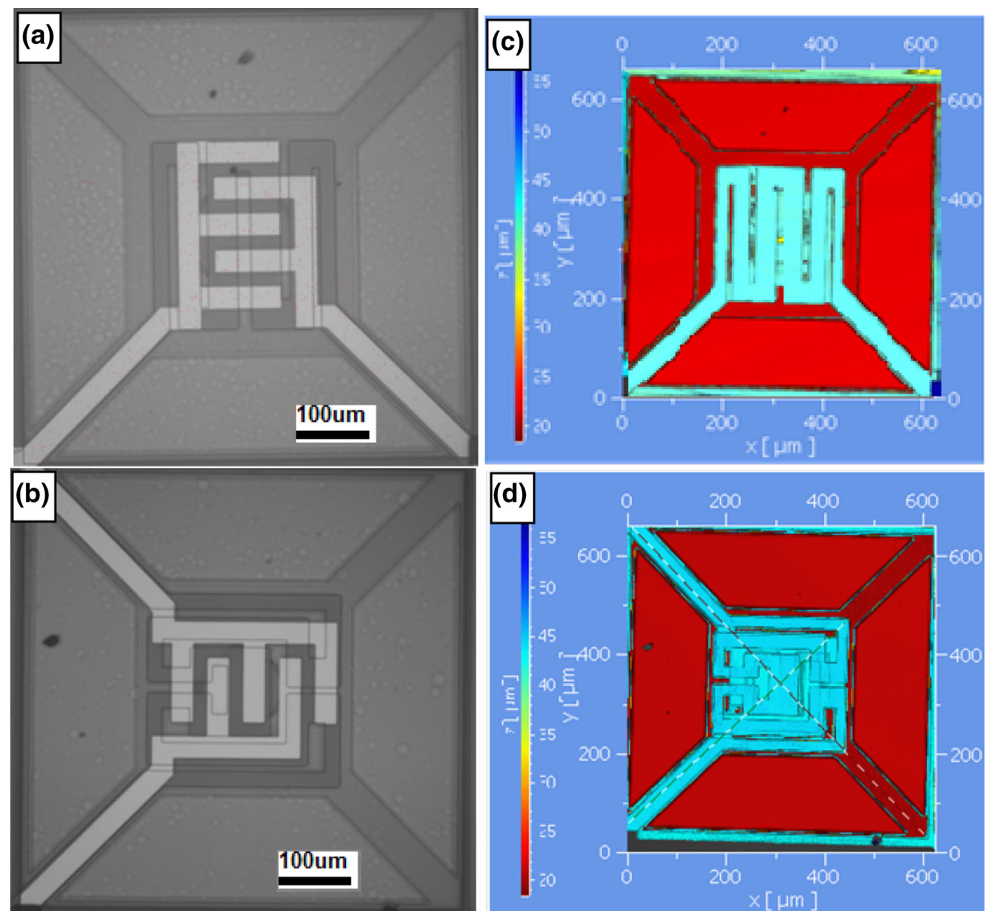

Fig. 2 CCD images of **a** serpentine and **b** fan shape heaters; 2D surface topography images of **c** serpentine and **d** fan shape heaters

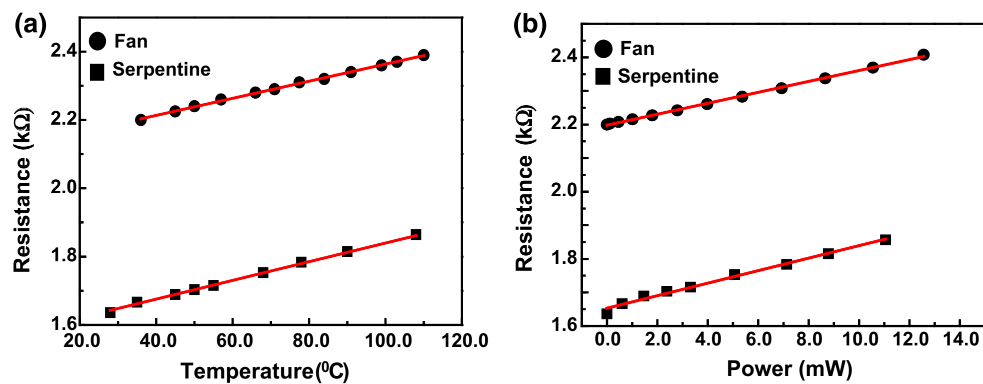

Fig. 3 **a** Heater resistance as a function of temperature when the MHPs were mounted on a heating stage. **b** Heater resistance as a function of applied power

fan shape heaters. The resistance data are then correlated to the corresponding temperatures using the TCR value to compute the thermal efficiency. From Fig. 3a, b, thermal efficiency of both the MHPs is determined as $\sim 10\ ^{\circ}C/mW$, which is higher as compared to other similar commercial sensor substrates (Weiller et al. 2004).

4 Temperature distribution study by thermal imaging of MHPs

Preliminary measurements of temperature profile of the MHPs are carried out by optical microscope (Olympus model BX63) by applying sufficient heater power such that the MHP glowed red-hot. Figure 4 shows the optical micrographs of serpentine and fan shape MHPs at an

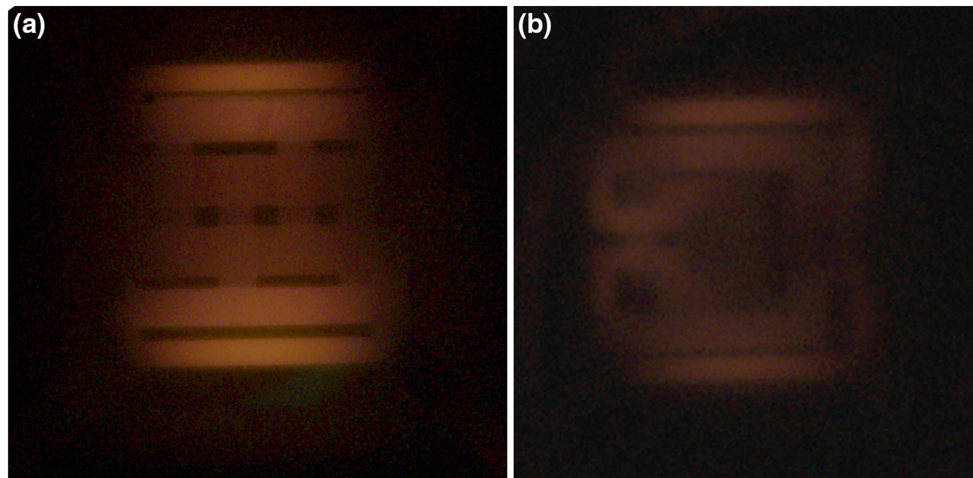

Fig. 4 Optical micrograph of **a** serpentine and **b** fan shaped MHPs; Heater power was 90 mW for the serpentine and 83 mW for the fan shape MHP

applied power of 90 and 83 mW respectively. As discussed above, by controlling the current density, the temperature of the outer part of the MHP is maintained higher in order to compensate for the heat loss due to conduction through the supporting beams.

The heating characteristics of the MHPs are further evaluated with a thermal imaging camera (Siver 420 from M/s CEDIP Infrared Systems, France). The camera uses high sensitivity InSb focal plane array detector in the spectral range between 3.6 and 5 µm. Figure 5 shows the thermal images of serpentine and fan shape MHPs for an applied heater power of 40 and 37 mW respectively. The average temperature of the active area comprising IDE is ~ 450 °C for both the MHPs. As seen from the exploded view of MHPs, more than 90% area of the suspended membrane is heated uniformly. Other than the suspended MHP, the remaining substrate stayed nearly at room temperature, resulting in localised heating. This is the major requirement of MHP based gas sensors.

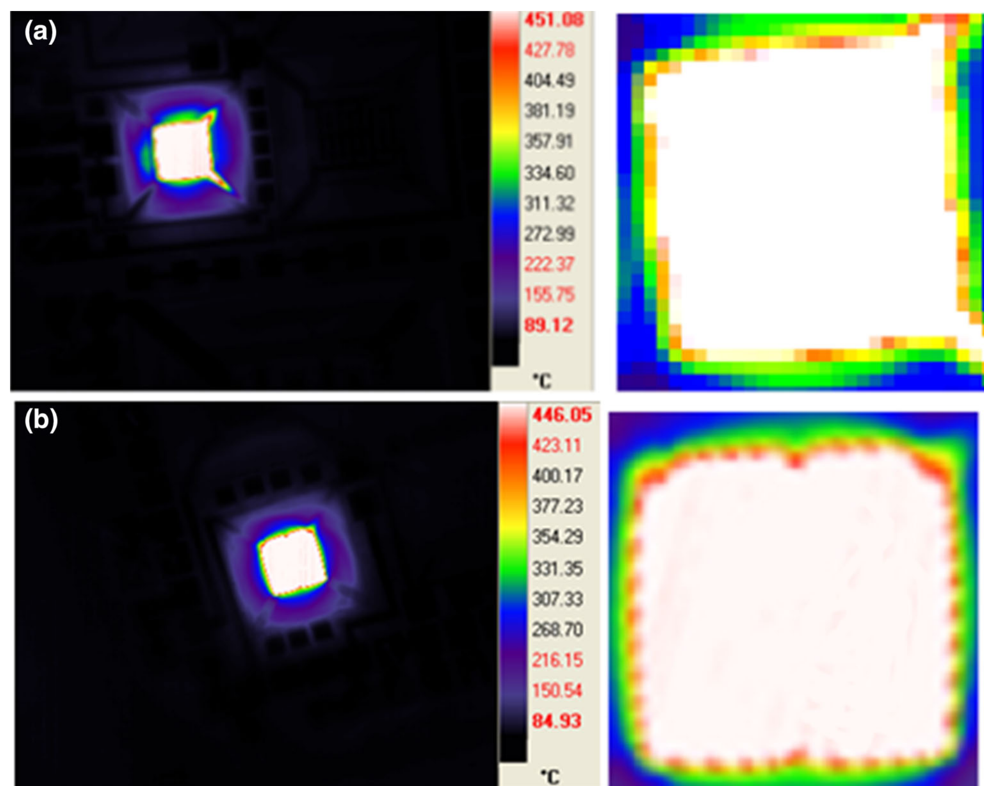

Fig. 5 Thermal camera images of **a** serpentine and **b** fan shape MHPs for an applied heater power of 40 and 37 mW respectively; figures on the right side show the expanded view of respective suspended membranes

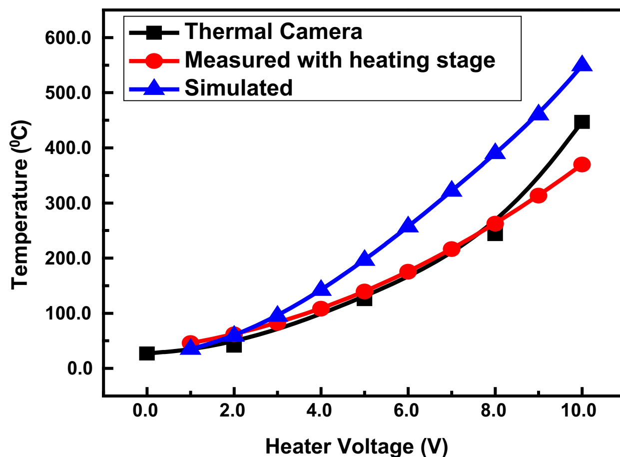

Fig. 6 Comparison of temperature characteristics evaluated by FEM simulation, electro-thermal measurements and thermal camera for serpentine heater MHP

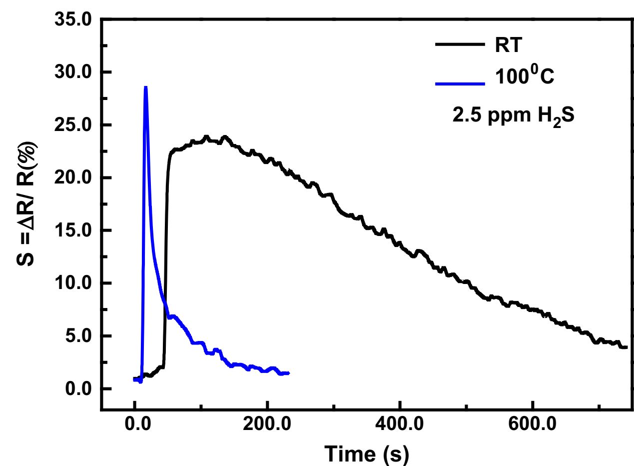

Fig. 7 H_2S sensing characteristics of RF sputtered SnO_2 thin film deposited on 300 μm × 300 μm MHP

Figure 6 shows the comparison of temperature characteristics as evaluated by FEM simulation, electro-thermal measurements and thermal camera for serpentine MHP. Similar results are obtained for fan shape MHP also. Though the simulation model took into account of MUMPs process details, complex effects such as geometric errors, damping, non-uniformities, residual stress, mismatching mask alignment, etc., during the fabrication are not accounted for in an idealized model. Hence there is a deviation of the simulated temperature curve at higher heater power compared to the experimental data. It is evident from Fig. 6 that there is a good agreement between the temperature characteristics as measured by thermal camera and as estimated from the heater resistance.

5 Gas sensing performance studies

Preliminary studies on gas sensing performance are carried out by depositing SnO_2 thin film by RF magnetron sputtering technique on the IDE of serpentine MHP chip (without any mask). Commercially available sintered SnO_2 target is used for sputtering at an RF power of 75 W and Ar:O_2 ratio of 1:1. Typical response curve of the MHP gas sensor for 2.5 ppm H_2S is shown in Fig. 7. When the sensor is exposed to H_2S, it interacts with the adsorbed oxygen species on the SnO_2 surface and injects the electrons back to the conduction band, thereby increasing the surface conductivity. As expected, the response kinetics are better at 100 °C compared to that at room temperature (Eranna et al. 2004). To further assess the sensor performance, suitable patterning method will be adapted to deposit sensing layer only on IDE and systematic studies will be carried out.

6 Conclusions

Surface micromachined MHPs based on MUMPs process have been designed for gas sensor applications. The FEM simulations confirmed that the MHPs showed good thermal isolation and homogeneous temperature distribution. The surface topography measurements verified that the X–Y–Z dimensions of the fabricated MHPs matched well with the design. From the temperature dependence of resistance, TCR of the polysilicon heater was estimated which in turn was used for computing the MHP temperatures at different input power. Optical microscopy and IR thermal imaging of the MHPs confirmed the temperature homogeneity on the suspended membrane. The IR thermal images affirmed that $> 90\%$ of the MHP showed uniform temperature of $\sim$ 450°C at < 40 mW heater power. The temperature characteristics as measured by thermal camera and as estimated from heater resistance matched well for both MHPs. These results suggest that MHPs based on MUMPs provide a cost effective solution for exploring various structures for MEMS based gas sensor applications.

Acknowledgements The authors would like to thank Prof. M. Deshmukh, TIFR for helping in wire-bonding the MHPs. The authors acknowledge the support extended by Mr. Philip Sebin and Mr. Arvind Kumar of Electronics Division, BARC in the characterization of MHPs.

References

Bhattacharyya P, Basu PK, Mondal B, Saha H (2008) A low power MEMS gas sensor based on nanocrystalline ZnO thin films for sensing methane. Microelectron Reliab 48:1772–1779

Briand D (2013) Micromachined semiconductor gas sensors. In: Jaaniso R, Tan OK (eds) semiconductor gas sensors. Woodhead Publishing Limited, Cambridge

Circuits Multi-Projects (2018). http://cmp.imag.fr. Accessed 25 Aug 2014

Eranna G, Joshi BC, Runthala DP, Gupta RP (2004) Oxide materials for development of integrated gas sensors—a comprehensive review. Crit Rev Solid State Mater Sci 29(3):111–118

Girija KG, Kaur D, Belwanshi V, Vatsa RK, Topkar A (2015) Design and electro-thermal analysis of micro hotplates for chemical sensors using standard multi user MEMS process. In: IEEE Xplore Proceedings of ISPTS-2, 7220075, pp 27–29

Girija KG, Tushir I, Vatsa RK, Topkar A (2017) Design, simulation and fabrication of piezoresistive microcantilevers using standard multi user MEMS process. ISSS J Micro Smart Syst 6:83–89

Graf M, Barrettino D, Kirstein K, Hierlemann A (2006) CMOS microhotplate sensor system for operating temperatures up to 500 °C. Sens Actuators B 117:346–352

Kumar A, Eranna G (2016) Design and electro-thermal analysis of surface micromachined perforated membrane hotplate for chemical gas sensor applications. Microsyst Technol 22:2559–2564

Li M, Zhu WYH, Guo Z, Tang Z (2015) Fabrication and characterization of a low power consumption ethanol gas sensor based on a suspended micro-hotplate. RSC Adv 5:51953–51960

Pal J, Zhu Y, Dao D, Lu J, Khan F (2015) RF MEMS switches for smart antennas. Microsyst Technol 21:487–495

Puigcorbe J, Vogel D, Michel B, Vila A, Gracia I, Cane C, Morante JR (2003) Thermal and mechanical analysis of micromachined gas sensors. J Micromech Microeng 13:548–556

Qu P, Qu H (2013) Design and characterization of a fully differential MEMS accelerometer fabricated using metalMUMPs technology. Sensors 13:5720–5736

Rao LLR, Singha MK, Subramaniam KM, Jampana N, Asokan S (2016) Molybdenum microheaters for MEMS-based gas sensor applications: fabrication. Electro Thermo Mech Response Char-act IEEE Sens J 17:22–29

Samaeifar F, Hajghassem H, Afifi A, Abdollahi H (2015) Implementation of high-performance MEMS platinum micro-hotplate. Sens Rev 35:116–124

Shakoor RI, Bazaz SA, Burnie M, Lai Y, Hasan MM (2011) Electrothermally actuated resonant rate gyroscope fabricated using the MetalMUMPs. Microelectron J 42:585–593

Simon I, Barsan N, Bauer M (2001) Micromachined metal oxide gas sensors: opportunities to improve sensor performance. Sens Actuators B 73:1–26

Spannhake J, Helwig A, Schulz O, Muller G (2009) Micro-fabrication of gas sensors, chapter 1. In: Comini E, Faglia G, Sberveglieri G (eds) Solid state gas sensing. Springer, Boston, MA

Vernieres J, Steinhauer S, Zhao J, Chapelle A, Menini P, Dufour N, Diaz RE, Nordlund K, Djurabekova F, Grammatikopoulos P, Sowwan M (2017) Gas phase synthesis of multifunctional Fe-based nanocubes. Adv Funct Mater 27:1605328

Wang L, Jin Y (2017) A push-pull double-contact MEMS relay fabricated by MetalMUMPs process. Microsyst Technol 23:2257–2262

Weiller BH, Fuqua PD, Osborn JV (2004) Fabrication, characterization, and thermal failure analysis of a micro hot plate chemical sensor substrate. J Electrochem Soc 151:H59–H65

Wöllenstein J, Plaza JA, Cane C, Min Y, Böttner H, Tuller HL (2003) A novel single chip thin film metal oxide array. Sens Actuators B 93:350–355